Available online at www.sciencedirect.com
SCIENCE DIRECT®
Composites: Part A 34 (2003) 743–753
composites
Part A: applied science and manufacturing
www.elsevier.com/locate/compositesa

Self-healing structural composite materials

M.R. Kessler[a,*], N.R. Sottos[c,d], S.R. White[b,d]

[a]Department of Mechanical Engineering, University of Tulsa, 600 South College Avenue, Tulsa, OK 74104, USA
[b]Department of Aerospace Engineering, University of Illinois at Urbana-Champaign, Urbana, IL 61801, USA
[c]Department of Theoretical and Applied Mechanics, University of Illinois at Urbana-Champaign, Urbana, IL 61801, USA
[d]Beckman Institute for Advanced Science and Technology, University of Illinois at Urbana-Champaign, Urbana, IL 61801, USA

Received 24 January 2003; revised 26 February 2003; accepted 18 March 2003

Abstract

A self-healing fiber-reinforced structural polymer matrix composite material is demonstrated. In the composite, a microencapsulated healing agent and a solid chemical catalyst are dispersed within the polymer matrix phase. Healing is triggered by crack propagation through the microcapsules, which then release the healing agent into the crack plane. Subsequent exposure of the healing agent to the chemical catalyst initiates polymerization and bonding of the crack faces. Self-healing (autonomic healing) is demonstrated on width-tapered double cantilever beam fracture specimens in which a mid-plane delamination is introduced and then allowed to heal. Autonomic healing at room temperature yields as much as 45% recovery of virgin interlaminar fracture toughness, while healing at 80 °C increases the recovery to over 80%. The in situ kinetics of healing in structural composites is investigated in comparison to that of neat epoxy resin.

Keywords: A. Polymer-matrix composites (PMCs); B. Delamination; B. Fracture toughness; E. Repair

1. Introduction

Brittle polymers and the structural composites made from them are susceptible to microcracking when subjected to repeated thermomechanical loading. For structural composites, these matrix microcracks coalesce and lead to other damage modes including fiber/matrix debonding and ply delamination [1–3]. Long-term degradation of material properties results and much effort is directed towards reliable damage prediction and property degradation models. This damage is difficult to detect and even more difficult to repair because it often forms deep within the structure. Once this damage has developed, the integrity of the structure is greatly compromised.

Currently, composite parts that have been damaged in service are first inspected manually to determine the extent of damage. For critical parts, this inspection may include non-destructive testing (NDT) techniques as ultrasonics, infrared thermography, X-ray tomography, and computerized vibro thermography [4]. If the damage is too severe the structural component is replaced entirely. For less extensive damage, repairs are attempted. If localized delamination has occurred it may be repaired by injecting resin via an access hole into the failed area. Another common repair method is the use of a reinforcing patch bonded or bolted to the composite structure. Numerous studies regarding these and other composite repair methods have been published [5–12], yet all require time-consuming and costly manual intervention by a trained technician.

Recently, a self-healing polymer was developed [13] that offers promise in significantly extending the life of polymeric components by autonomically healing microcracks whenever and wherever they develop. The concept is shown in Fig. 1 in which healing is accomplished by incorporating a microencapsulated healing agent and catalytic chemical trigger within an epoxy matrix. An approaching crack ruptures embedded microcapsules releasing healing agent into the crack plane through capillary action. Polymerization of the healing agent is triggered by contact with the embedded catalyst, bonding the crack faces. This approach has yielded remarkable performance in neat resin samples where ca. 90% recovery of virgin fracture toughness is achieved [14].

Transitioning these promising results from neat resins to structural (fiber-reinforced) composites is challenging.

* Corresponding author. Tel.: +1-918-631-3056; fax: +1-918-631-2397.
E-mail address: michael-kessler@utulsa.edu (M.R. Kessler).

1359-835X/03/$ - see front matter © 2003 Elsevier Ltd. All rights reserved.
doi:10.1016/S1359-835X(03)00138-6

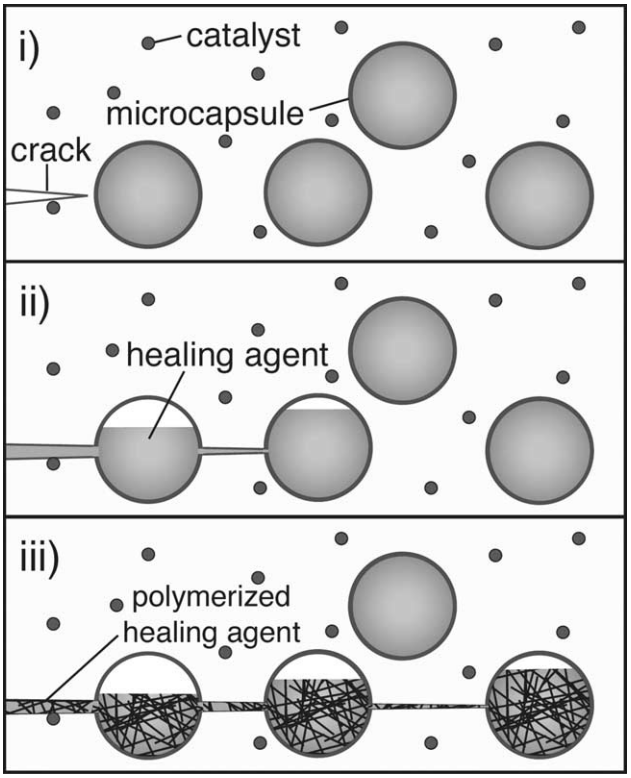

Fig. 1. The self-healing concept [13]. A microencapsulated healing agent is embedded in a structural composite matrix containing a catalyst capable of polymerizing the healing agent. (i) Cracks form in the matrix wherever damage occurs. (ii) The crack ruptures the microcapsules, releasing the healing agent into the crack plane through capillary action. (iii) The healing agent contacts the catalyst, triggering polymerization that bonds the crack faces closed.

Previously, it was shown that healing of delaminations could be self-activated by incorporating the same catalytic trigger within the matrix of a fiber-reinforced composites [15]. In situ polymerization kinetics was shown to play a crucial role in determining the degree of repair achieved. Here, we demonstrate a fully self-healing structural composite system utilizing the concept shown in Fig. 1. The focus of this study is the repair of delamination damage in double cantilever beam (DCB) specimens.

2. Experimental methods

2.1. Materials

There are several constituent materials which, when combined, function as a self-healing materials system: healing agent, microcapsule shell, chemical catalyst, polymer matrix, and fiber-reinforcement. The healing agent used in this study was dicyclopentadiene (DCPD) monomer which possesses low viscosity and excellent shelf life when stabilized with 100–200 ppm *p-tert*-butylcatechol. The healing agent was encapsulated in poly-urea-formaldehyde by in situ polymerization [13] to yield

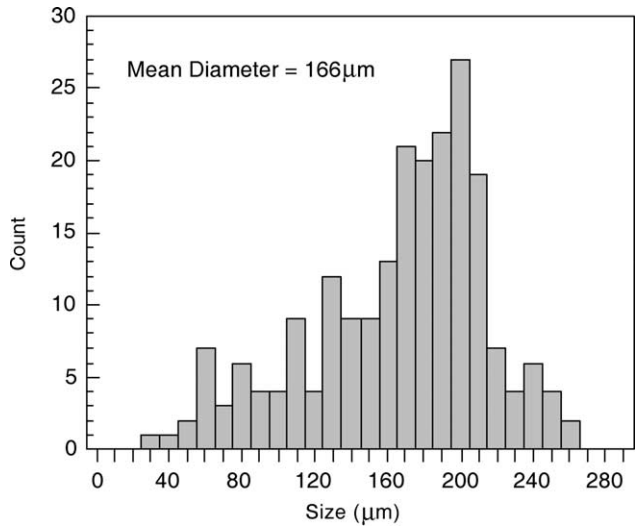

Fig. 2. Size distribution of microcapsules of DCPD prepared by the in situ polymerization technique and used in the manufacture of composite panels.

microcapsules with a mean diameter of 166 μm. Fig. 2 shows a typical size distribution of microcapsules from the in situ polymerization process.

The catalyst that was used is bis(tricyclohexylphosphine)benzylidine ruthenium (IV) dicholride (Grubbs' catalyst). Grubbs' catalyst initiates a ring-opening-metathesis-polymerization (ROMP) of DCPD and produces a tough, highly cross-linked polymer. Thermal decomposition of Grubbs' catalyst occurs above 120 °C as determined by DSC analysis [16].

An epoxy polymer matrix (EPON 828, Miller–Stephenson Chemical Co.) was used to fabricate the composite materials used in this study. In the previous work [16], it was shown that exposure of Grubbs' catalyst to a primary amine curing agent leads to some degradation of chemical activity of the catalyst. Although adjusting mixing order and curing time can mitigate this degradation, alternative curing agents were investigated for this study. A tertiary amine system (Ancamine K54, Air Products and Chemicals) was selected that shows little chemical interaction with Grubbs' catalyst. A high molecular weight epoxy flexiblizer (Heloxy 71, Shell Chemical Company) was added to the formulation to improve the toughness of the matrix and to improve subsequent crack growth stability.

Carbon fiber-reinforcement was used to form a structural composite material. The fiber was incorporated in the form of a plain weave fabric (Fibre Glast Development Corp.) constructed with 3 K tows in a 12.5 × 12.5 (tpi) plain weave architecture yielding plies with 193 g/m^2 arial weight.

2.2. Composite panel manufacturing

Composite panels were manufactured by hand lay-up and compression molding. Sixteen 305 mm × 230 mm rectangles were cut from the carbon fabric and the edges

were taped with 25 μm polyester tape (Airtech International) to prevent fraying of the fabric.

Epon 828 was then mixed with Heloxy 71 flexibilizer at a concentration of 5:3 (by wt) epoxide to flexibilizer. Ancamine K54 was added at a concentration of 10:100 (by wt) curing agent to the epoxide–flexibilizer mixture. For some of the samples, a portion of the resin was set aside and used for impregnation of the central fourfabric layers. Into this portion of the resin was mixed 5 wt% Grubbs' catalyst, which was first ground with a mortar and pestle in a nitrogen filled glove box. For self-healing samples DCPD-filled microcapsules were slowly mixed with the resin at a concentration of 20 wt% before it was used to impregnate the central fabric layers. Next, the resin was degassed in a vacuum chamber for approximately 15 min to thoroughly remove entrapped air bubbles.

During panel lay-up the first six (of 16) carbon fabric plies were impregnated with the unfilled resin mixture using a hard plastic applicator. The resin for the next four fabric layers was applied with a 50 mm brush to prevent rupture of the microcapsules during resin application. In the middle of these four layers, a 13 μm thick Teflon® film (Norton Performance Plastics) was placed to create the initial delamination crack. The final six plies were impregnated and stacked on top to create a 16-ply panel. The panel was then placed between two aluminum plates covered with release film and compressed in a tetrahedron (MTP-14) hot press at 2225 N (yielding 31.7 kPa compaction pressure) at 25 °C for 24 h. Cured panels were then placed in an oven for post cure at 30 °C for 48 h. The resulting panels had a nominal thickness of 6 mm after cure.

2.3. Fracture specimens

In laminated composites and adhesives the DCB specimen is commonly used to measure interlaminar fracture toughness. For many materials and testing conditions it is particularly difficult to measure crack length and in these cases it is desirable that the energy release rate remains constant with crack length. By contouring the width of the standard DCB specimen appropriately, the energy release rate becomes independent of crack length. These width-tapered (WTDCB) specimens, first introduced by Mostovoy [17,18] have been used by a number of investigators to measure Mode I interlaminar fracture toughness [19–28]. By applying standard beam mechanics to the specimen sketched in Fig. 3 (neglecting the untapered regions) together with linear elastic fracture mechanics of the delamination along the mid-place, the stress intensity factor of the specimen can be expressed as

$$K_{\mathrm{I}} = 2Pk\sqrt{\frac{3}{(1-\nu^2)h^3}} \tag{1}$$

where P is the applied load, k is the taper ratio (a/b), h is the specimen half-thickness, and ν is the Poisson's ratio. The only unknown variable in this equation is P and the fracture toughness can therefore be directly related to the critical load measured during crack propagation. This equation

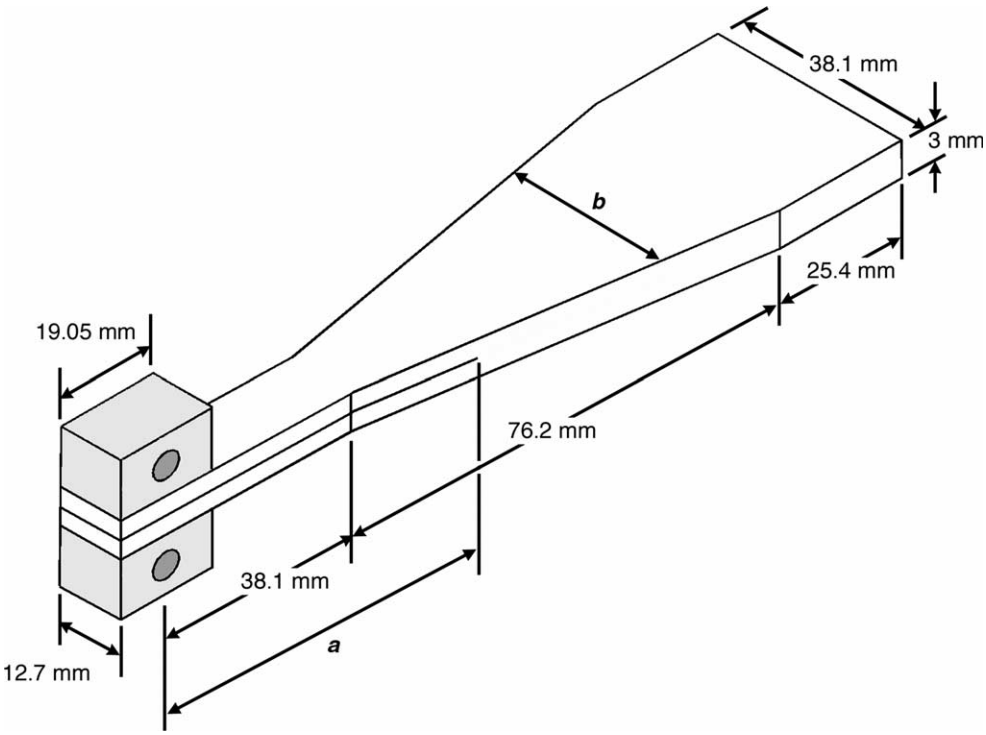

Fig. 3. Geometry of the WTDCB specimen used in the fracture experiments. A Teflon® insert is included to initiate a delamination along the specimen midplane of length a. A non-tapered region (25.4 mm) at the end of the specimen is included for crack arrest.

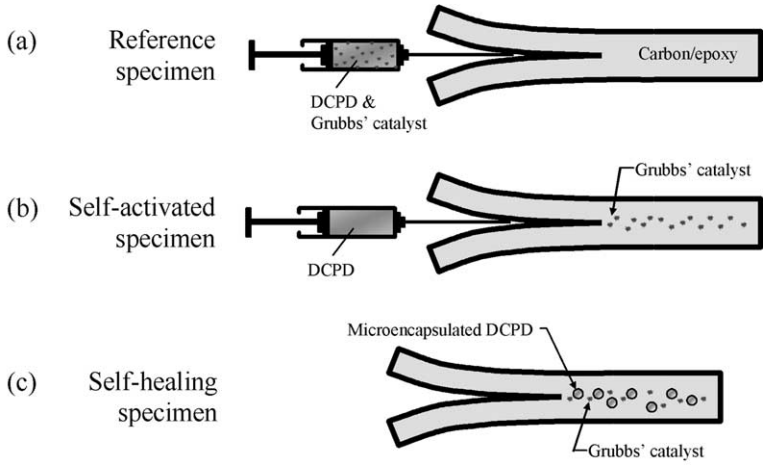

Fig. 4. The three types of WTDCB specimens tested. (a) Reference specimen in which the healing agent is manually catalyzed and then injected into the delamination. (b) Self-activated specimen where the catalyst is embedded within the polymer matrix and the healing agent is manually injected into the delamination. (c) Self-healing specimen in which microcapsules of the healing agent and the catalyst are embedded into the polymer matrix and healing is autonomic.

holds for specimens in which the bending stiffness is large enough to substantiate the assumptions of 1D beam mechanics and for regions removed from the end of the specimen where edge effects begin to dominate. For the present case a non-linear finite element study was performed to validate the use of Eq. (1) for the material system investigated.

Composite panels were machined into the WTDCB geometry shown in Fig. 3 yielding 6–7 specimens per panel. The Teflon® insert extended for approximately 60 mm along the midplane of the specimen. Two steel loading blocks with through-holes for loading pins were bonded to the end of each specimen with an epoxy adhesive (Epoxy 907, Miller–Stephenson Chemical Company).

A region of non-tapered length (25.4 mm) at the end of the specimen was included as a crack arrest region to prevent the specimen from breaking completely into two pieces in the event of unstable crack growth. The additional length is not believed to influence the behavior of the specimen for crack lengths less than 105 mm.

Three different types of specimens were manufactured, as shown in Fig. 4. Reference and self-activated specimens were introduced in Ref. [15] and serve as experimental controls. Healing in these specimens involves some form of manual intervention, either injection of the healing agent (self-activated specimens) or catalyzation and injection of the healing agent (reference specimens). For self-healing specimens, microcapsules and catalyst are directly embedded in the matrix material and healing occurs autonomically without manual injection.

Five groups of samples were tested as shown in Table 1: one set of reference specimens, one set of self-activated specimens, and three different sets of self-healing specimens. One group of self-healing specimens was healed at an elevated temperature to measure the influence of temperature on healing efficiency. While healed tests for most specimens were conducted after more than 48 h post-fracture, specimens from one group were tested at nine different times after the virgin loading from 10 min to 48 h.

2.4. Testing procedure

WTDCB specimens were loaded in displacement control at 5 mm/min in a calibrated MTS load frame (Alliance RT/30) equipped with a 444.8 N load cell (Transducer Techniques) using pin loading. In the initial virgin loading cycle, the specimen was loaded until the crack approached the end of the tapered region ($a = 100$ mm). Load (P) and load-point displacement (δ) were recorded throughout the test using MTS TestWorks® software (V. 4.05B). For the reference specimens, 3 ml of DCPD was manually mixed with 30 mg of Grubbs' catalyst and injected using a syringe into the delamination with the crack fully open at the end of the virgin loading cycle (typically less than 1 ml was needed to adequately cover the crack plane). For the self-activated specimens, only

Table 1
Specimen types investigated

Variable	Specimen type	No.	Catalyst (%[a,b])	Capsules (%[a,b])	Healing conditions	
					Time (h)	Temp.
	Reference	6	0	0	24	RT[c]
Catalyst	Self-activated	6	5	0	>48	RT
Microcapsules	Self-healing	8	5	20	>48	RT
Temperature	Self-healing	4	5	20	>48	80 °C
Time	Self-healing	9	5	20	0–48	RT

[a] By weight.
[b] Resin used to impregnate central four plies of laminate.
[c] Approximately 25 °C.

pure DCPD was injected into the delamination, since the Grubbs catalyst had been incorporated previously into the central layers of each specimen. For the self-healing specimens, no manual intervention took place. Subsequently, all specimens were immediately unloaded and held closed with bar clamps (Quick–Grips®, American Tool). After a period of healing (typically 48 h unless otherwise noted) the specimens were reloaded to failure again while recording load and displacement.

2.5. Data reduction

A typical virgin load–displacement curve is shown in Fig. 5 The behavior is linear up to the onset of crack growth (at about 49 N). Upon further displacement, the crack advances along the specimen midplane in short, unstable jumps and arrests as reflected in the jagged load–displacement curve (such stick-slip crack propagation is common in brittle composites [29–32]). Initiation toughness values are determined from the peak loads prior to unstable fracture as revealed by the sudden drop in the load level in the load–displacement curve.

The degree of healing can be quantified by the healing efficiency, which for the WTDCB specimen is equal to the ratio of the critical loads necessary to propagate a crack through the healed and virgin material,

$$\eta = \sqrt{\frac{G_{IC}^{Healed}}{G_{IC}^{Virgin}}} = \frac{K_{IC}^{Healed}}{K_{IC}^{Virgin}} = \frac{P_C^{Healed}}{P_C^{Virgin}} \quad (2)$$

For a given sample there are multiple values for P_C and hence K_{IC}. An average healing efficiency for a given sample can be defined by the ratio of the average of all critical load values for the healed and virgin cases

$$\eta_{avg} = \frac{\text{Average}[P_C^{Healed}]}{\text{Average}[P_C^{Virgin}]} \quad (3)$$

whereas the maximum healing efficiency is based on the maximum critical load in the healed specimen, i.e.

$$\eta_{max} = \frac{\text{Max}[P_C^{Healed}]}{\text{Average}[P_C^{Virgin}]} \quad (4)$$

The discrepancy between the average and maximum healing efficiencies is reflective of variations in the degree of healing within regions of the sample due for example to uneven coverage of the fracture plane with healing agent or local variation in catalyst exposure. The quantities η_{avg} and η_{max} for each specimen in a group are then averaged and compared across groups to evaluate how material components or healing conditions influence healing efficiency.

3. Experimental results

3.1. Experimental controls

3.1.1. Reference specimens

The reference specimens serve as an experimental control and provide an upper bound for the potential degree of healing in a fully self-healing system. The healing agent is mixed with the catalyst and then manually injected into the delamination area. Delivery of the healing agent and chemical triggering of polymerization are optimal under these conditions and the degree of healing that is achieved is maximized.

Fig. 6 shows a typical load–displacement curve for a reference WTDCB specimen for both the virgin and healed tests. At the end of the virgin loading cycle the crack has propagated along the specimen midplane from the initial point (corresponding to the initial Teflon® insert) to a point near the end of the tapered region. While the specimen is still fully opened ($\delta = 32$ mm) the catalyzed healing agent is injected into the delamination with a syringe and the specimen is quickly unloaded, clamped closed, and allowed to heal. Upon retesting, the loading curve for the healed specimen follows the original loading curve until crack propagation begins anew at $P \sim 40$ N. Crack advancement

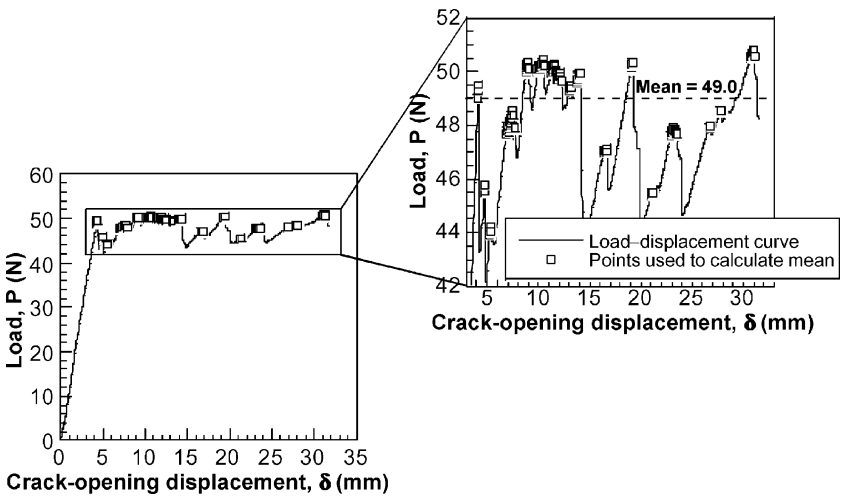

Fig. 5. Data reduction procedure for WTDCB tests to obtain the average fracture toughness from load–displacement data.

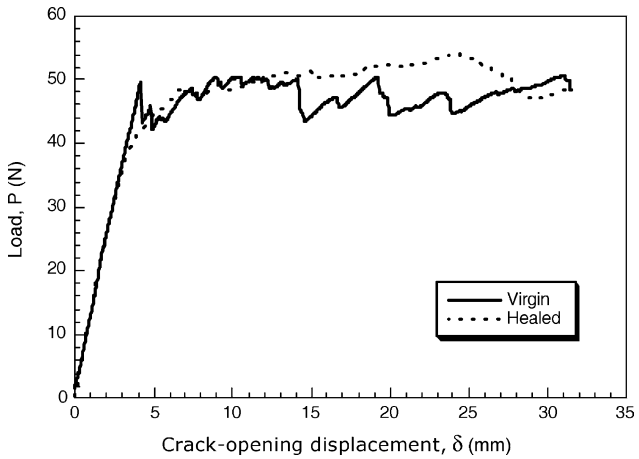

Fig. 6. Typical loading curves for virgin and healed reference specimens. [Note: unloading curves not shown.]

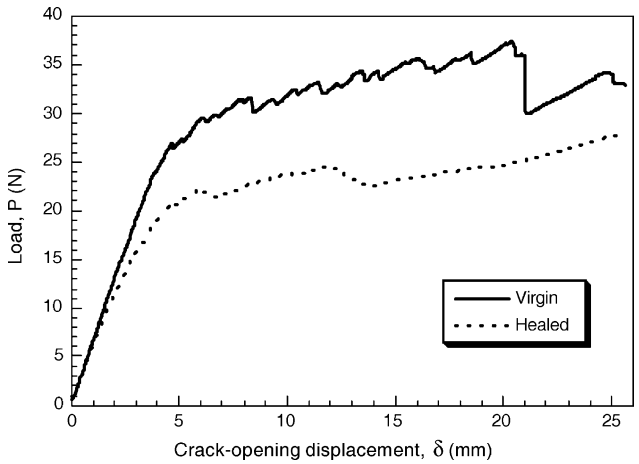

Fig. 7. Typical loading curves for virgin and healed self-activated specimens. [Note: unloading curves not shown.]

then occurs through the healed delamination region. One interesting feature of the results is the stable and continuous crack growth of the healed specimen compared to the erratic stick-slip crack growth through the virgin material.

While the initial crack growth begins earlier for the healed case when compared to the virgin loading cycle, the maximum load is actually higher during crack advancement. The healing efficiencies for the specimen shown in Fig. 7 based on Eqs. (3) and (4) are $\eta_{avg} = 101\%$ and $\eta_{max} = 111\%$. As shown in Table 2, the average of all the reference specimen tests yield $\eta_{avg} = 99\%$ and $\eta_{max} = 107\%$.

3.1.2. Self-activated specimens

The self-activated control specimens provide evidence that the embedded catalyst remains active after manufacturing of composite panels and is still capable of triggering ROMP of the healing agent. Delivery of the DCPD healing agent is performed manually by injection into the delamination area.

Typical virgin and healed load–displacement curves for a self-activated WTDCB specimen are shown in Fig. 7. The virgin loading curve exhibits stick-slip behavior while the healed loading curve is stable and continuous, as in the reference samples. The load values are noticeably lower than in the reference case indicating a decrease in the inherent toughness of the self-activated specimens. The average of all tests for self-activated specimens yields $\eta_{avg} = 73\%$ and $\eta_{max} = 82\%$.

Since the delivery of healing agent to the delamination is optimal and manually controlled in the self-activated specimens, the decrease in healing efficiency from that of the reference case is due solely to issues associated with interaction of the catalyst and healing agent at the fracture plane. If the rate of polymerization of the healing agent is slow compared to the bulk (reference case), some diffusion of the healing agent into the epoxy matrix can occur and incomplete coverage of the fracture plane results in a lower healing efficiency. Retardation of in situ kinetics may occur if the local concentration of catalyst exposed on the fracture plane is low (through preferential failure along the fiber/matrix interface for example). Further, evidence for the retardation of in situ healing kinetics is provided in the discussion of the results in Section 3.5.

3.2. Self-healing specimens

Reference control specimens established that the healing agent is capable of achieving high levels of repair in the composite material. Self-activated controls demonstrated that the embedded catalyst is capable of polymerizing the healing agent. Self-healing specimens represent the final synthesis of the concept into a fully integrated system that repairs the delamination autonomically.

Fig. 8 shows typical loading curves for a self-healing specimen with 20 wt% microcapsule concentration. In the virgin loading cycle, the load reaches a peak of about 45 N. In this particular specimen, at a displacement of about

Table 2
Summary of WTDCB test results

Specimen type	No. of samples	K_{IC} virgin avg. (MPa $m^{1/2}$)	K_{IC} healed avg. (MPa $m^{1/2}$)	K_{IC} healed peak (MPa $m^{1/2}$)	η_{avg} avg. (%)	η_{max} avg. (%)
Reference	6	3.58 (0.22)[a]	3.54 (0.14)	3.82 (0.20)	99	107
Self-activated	6	2.54 (0.12)	1.86 (0.09)	2.09 (0.13)	73	82
Self-healing (at room temp.)	8	2.85 (0.22)	1.08 (0.20)	1.29 (0.25)	38	45
Self-healing (at 80 °C)	4	2.79 (0.30)	1.83 (0.20)	2.23 (0.18)	66	80

[a] ± 1 standard deviation.

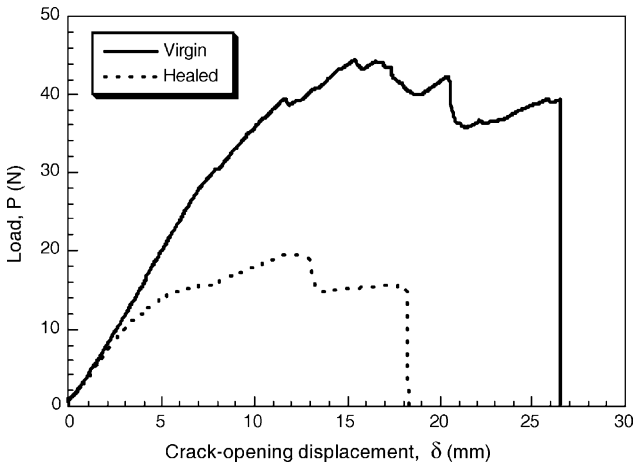

Fig. 8. Typical loading curves for virgin and healed self-healing. [Note: Healing conditions = 48 h at room temperature.]

26.5 mm, the delamination suddenly propagated to the end of the specimen and the load dropped to zero. The displacement was returned to zero and the two halves of the specimen were clamped back together and allowed to heal for 48 h. The subsequent reloading curve (healed) reached a maximum load of 19.5 N before the specimen ultimately broke in two pieces at a displacement of about 18 mm. Of the eight specimens tested, three fractured completely before the test was halted; however, there was no detectable correlation between healing efficiency and whether the specimen broke completely in the initial loading. The average of all the healing efficiencies for self-healing specimens after healing at room temperature for 48 h are $\eta_{avg} = 38\%$ and $\eta_{max} = 45\%$.

A typical virgin fracture surface for a self-healing specimen is shown in Fig. 9 Where the fracture is primarily interfacial between the fiber and the matrix (bottom right of the image), there are few observable broken microcapsules. In regions where crack propagation was confined to the matrix (top left of the image) there are multiple broken microcapsules present.

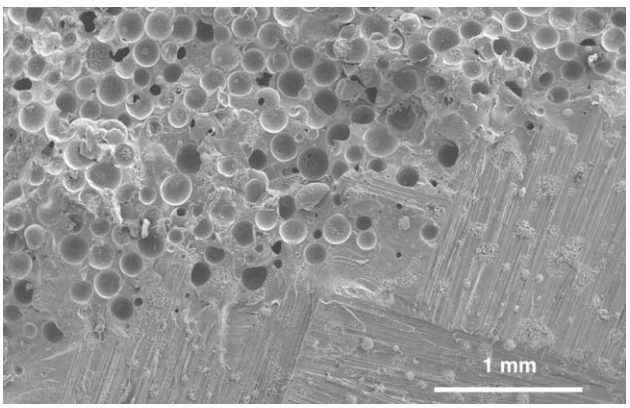

Fig. 9. Scanning electron microscope image of the fracture surface after virgin testing of a self-healing specimen.

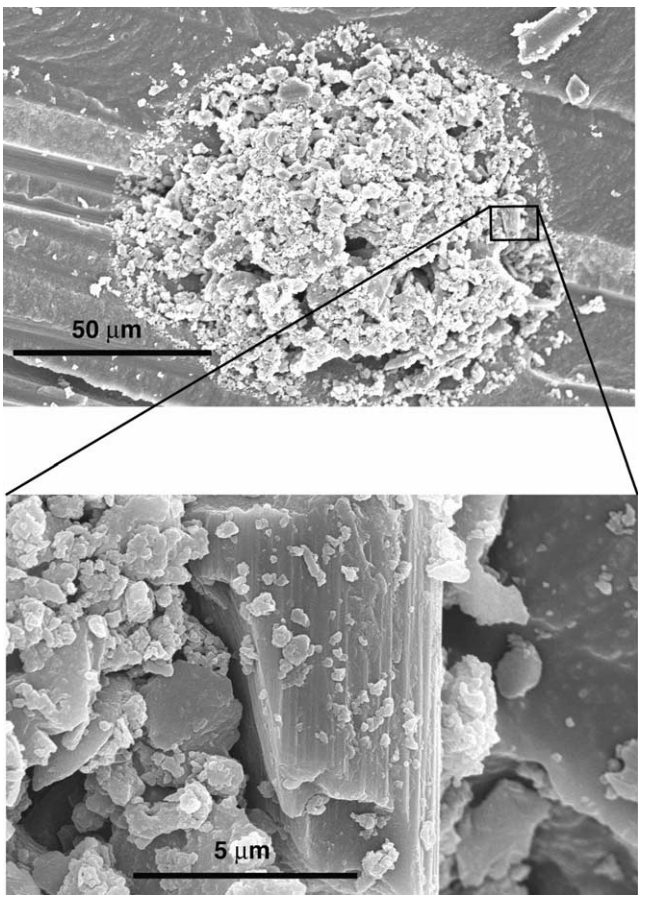

Fig. 10. Scanning electron microscope image of the fracture surface after virgin testing of a self-healing specimen showing catalyst particle clustering.

Catalyst clusters are also apparent on the fracture plane. Fig. 10 shows two magnifications of a cluster of Grubbs' catalyst along with debris from the failure of the specimen. These catalyst clusters and the high concentrations of microcapsules in the matrix are likely contributing factors in unstable crack propagation in the virgin loading cycle (Fig. 8).

A cross-sectional view of a self-healing specimen is shown in Fig. 11 The central layers, which contain the microcapsules and catalyst, are significantly thicker than the surrounding layers. The average thickness of the central four layers in Fig. 11 is 0.58 mm, while the average layer thickness for the reference control specimens is 0.36 mm. This increased thickness of the interlaminar region may be the controlling factor in the reduction of virgin toughness compared with the reference controls [33,34].

3.3. Influence of temperature on self-healing

Based on analysis of the cure kinetics of the ROMP of DCPD in Ref. [35], we expect the temperature at which the samples are healed to greatly influence the healing efficiency. Healing at an elevated temperature increases

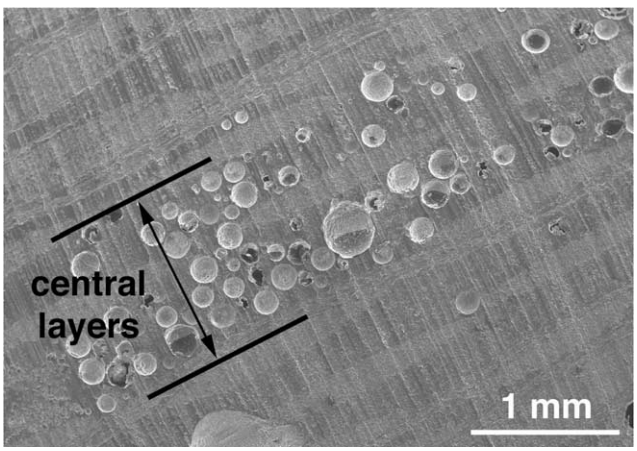

Fig. 11. Scanning electron microscope image of the cross-section of a self-healing specimen.

both the rate of polymerization and the ultimate degree of cure for the healing agent. By increasing the rate of polymerization, there is less chance for the healing agent to evaporate or diffuse away from the crack plane. Additionally, a higher degree of cure results in a polymerized healing agent with superior mechanical and adhesive properties.

The virgin and healed loading curves for a self-healing specimen that was allowed to heal at 80 °C for 48 h are shown in Fig. 12. The virgin loading is characterized by two large load drops, which correspond to rapid crack advancement through the mid-plane. A peak load of 42 N occurs just before the initial unstable crack propagation. The final load drops to zero when the delamination propagates to the end of the specimen. The specimen was then clamped shut and placed in an 80 °C oven. The subsequent loading curve results in a peak load of 33 N, nearly 1.7 times higher than the peak healed load in Fig. 8, where an identical specimen (same batch) was healed at room temperature.

The average of all the healing efficiencies for the self-healing specimens healed at 80 °C are $\eta_{avg} = 66\%$ and $\eta_{max} = 80\%$. Clearly, an elevated healing temperature increases the overall healing efficiency of the self-healing material. The group average healing efficiency, whether measured by the specimen-average critical load (η_{avg}) or by the specimen-maximum critical load (η_{max}), is nearly 1.7 times higher when the specimens were healed at 80 °C than when they were allowed to heal at room temperature.

As a control experiment, neat DCPD was injected into a delaminated reference specimen and the specimen was clamped shut and placed in the 80 °C oven. After 48 h when the specimen was removed from the oven, the specimen showed no evidence of healing and was unable to carry load.

3.4. In situ healing kinetics

A conservative healing period of 48 h was used for all tests to ensure full healing at room temperature conditions. From independent studies of the cure kinetics of the healing agent [35], it is clear that the in situ cure time will depend on both the local catalyst concentration and the temperature at which healing occurs. The time-dependent development of healing efficiency at room temperature was measured for one set of nine specimens manufactured from the same batch. Each specimen was allowed to heal for varying amounts of time from 10 min to 48 h. The resulting healing efficiencies are plotted versus log time in Fig. 13. Initially, no measurable healing could be detected until $t_{heal} > 30$ min, a time which correlates closely to the gel time at room temperature [35] and with the in situ kinetics of the neat resin [14]. As the healing time increases, the healing efficiency increases rapidly until reaching a maximum at $t_{heal} = 48$ h.

While performing the experiments on specimens that had been allowed to heal for 0.5–2.5 h, partially cured DCPD strands were observed bridging the crack behind the crack tip. Scanning electron microscopy of the fracture surface of a specimen where $t_{heal} = 0.5$ h is shown in Fig. 14. Present

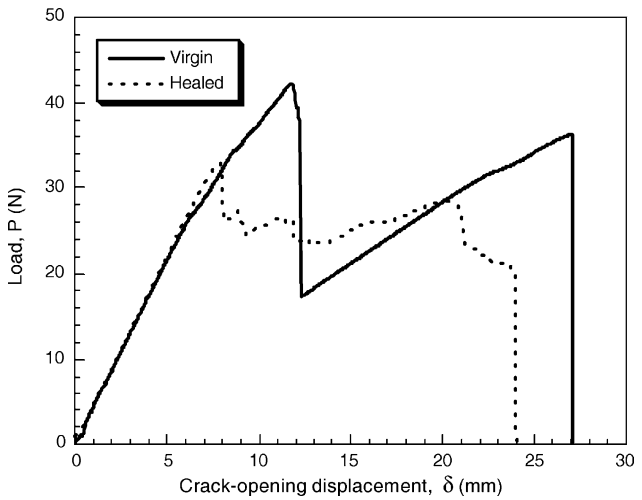

Fig. 12. Typical loading curves for virgin and healed self-healing specimens. [Note: Healing conditions = 48 h at 80 °C.]

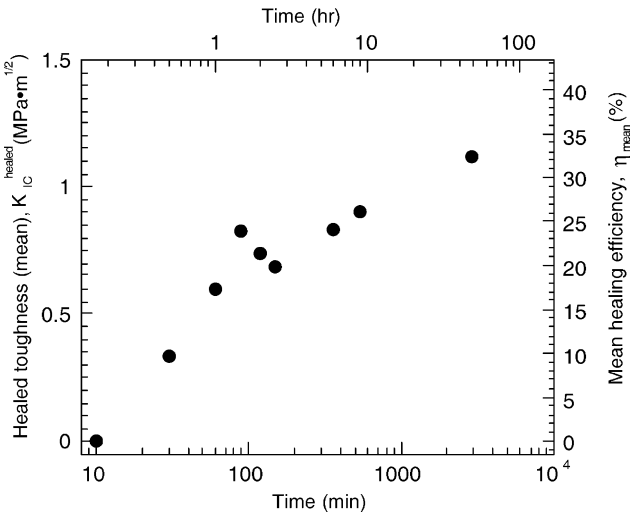

Fig. 13. Healed fracture toughness and healing efficiency vs. log healing time at room temperature for self-healing specimens.

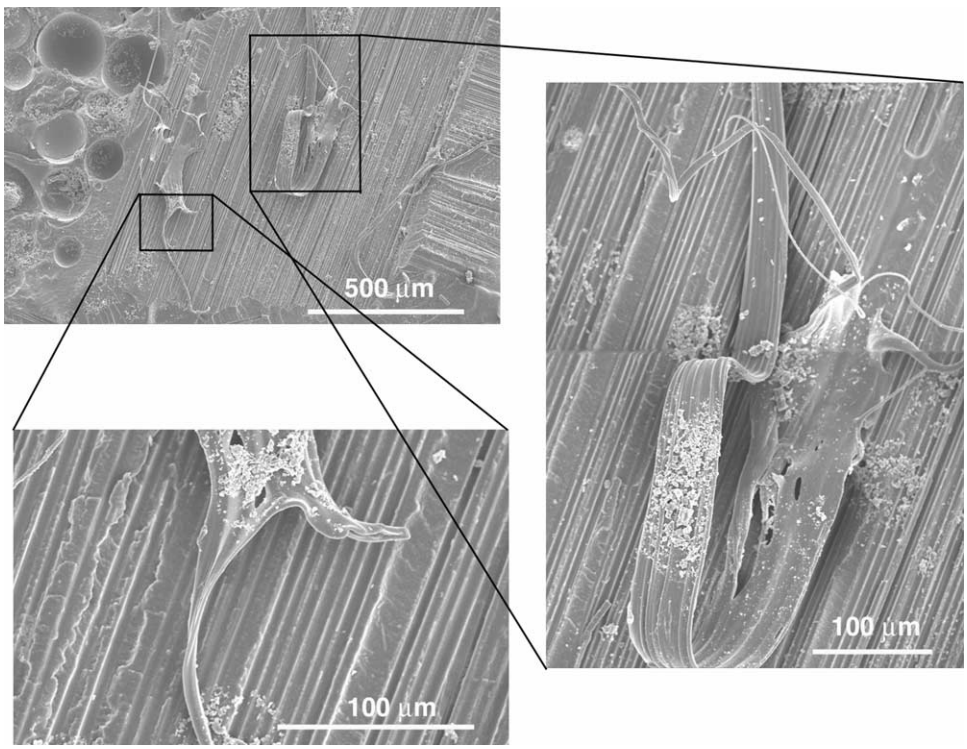

Fig. 14. Scanning electron microscope image of the healed fracture surface of a self-healing specimen tested after 30 min healing time.

on the surface are several strands of poly(DCPD) that bridged the two surfaces of the delamination before ultimately rupturing and collapsing in a folded film on the fracture surface.

3.5. Discussion of results

The recovery of interlaminar fracture toughness in a delaminated self-healing structural composite is accomplished at room temperature in an autonomic fashion. With no manual intervention a recovery of nearly 50% is achieved. Upon elevating the temperature slightly to 80 °C, healing efficiency is dramatically increased to over 80%. This dependence on healing temperature indicates that the healing efficiency is quite sensitive to temperature and by inference, the in situ kinetics of curing. While experiments on the self-healing matrix have shown ca. 90% recovery at room temperature conditions [14], the structural composite version presented in this paper contains a high thermal mass of reinforcing fibers and a lower mass fraction of self-healing matrix. Both can contribute to a lower local temperature at the crack face where healing is initiated. Since the ROMP is an exothermic reaction, local temperatures at the crack face may be slightly higher than room temperature during healing. In this case, the composite system would be expected to show a slightly lower temperature during healing and thus, a retardation of in situ healing kinetics. By analyzing Fig. 13 and the corresponding data of the epoxy matrix [14] the time constant of the initial healing curve yields 7.71 h^{-1} for the composite versus 6.43 h^{-1} for the matrix alone, a retardation of about 20%. Interestingly, the self-heating that occurs naturally in polymers and polymer matrix composites during fatigue may prove to be beneficial in accelerating the in situ cure kinetics and yield higher healing efficiencies.

The reduction in virgin interlaminar toughness for the self-healing composite material is believed to be due to two affects: (1) increased interlaminar thickness due to size and concentration of microcapsules, and (2) catalyst dispersion. High microcapsule concentration (20 wt%) was used to assure that adequate healing agent was available at the site of the delamination. As a result, the viscosity of the resin that was used in the central four layers of the composite lay-up was quite high and it was difficult to apply the resin with a single layer of capsules. The average thickness of the central layers was almost 60% higher than the outer layers (which did not contain catalysts and microcapsules). It is well known that the increased thickness of the interlaminar region leads directly to lower toughness. As a preliminary investigation of this affect we tested samples that contained 10 wt% microcapsules in the resin for the central layers and found that the virgin toughness was increased 21% to 3.45 MPa $m^{1/2}$. This shows that the high loading of microcapsules is responsible for part of the reduction in virgin toughness.

Self-activated specimens which contained the catalyst alone also showed a reduction in virgin toughness. Post-fracture observations of the delamination plane revealed evidence of agglomeration of catalyst particles (Fig. 10).

While the bonding to the catalyst particles is quite good, the core of the particle clusters is largely dry and indicates that the resin was not able to infiltrate these clusters. Consequently, these clusters are weak in the fracture plane and lead to a lowering of the virgin toughness. By lowering the catalyst concentration and improving the dispersion of the catalyst prior to composite lay-up these effects can be mitigated. In addition, other methods of dispersing the catalyst could prove beneficial such as attaching the catalyst to the surface of the fiber or of the microcapsule itself.

Realizing that the matrix resin has been shown to be significantly toughened (up to 127%) by the addition of microcapsules [13,14] and, to a lesser extent, by the addition of the catalyst phase [14], a toughened structural composite material should be achievable with refinement of the manufacturing and processing techniques. In Ref. [14] a maximum toughness in a neat epoxy matrix system was achieved at 15 wt% capsule concentration with SEM micrographs indicating a crack pinning toughening mechanism.

4. Conclusions

A new structural fiber-reinforced polymer matrix composite material has been demonstrated that can autonomically heal delaminations at room temperature, i.e. self-heal. Width-tapered DCB specimens were manufactured by hot pressing of woven graphite fiber preform and an epoxy matrix. The central layers where the delamination was introduced were filled with 20 wt% microcapsules of a monomeric healing agent of DCPD and 5 wt% of a ROMP catalyst (Grubbs' catalyst). Freshly fractured specimens were clamped shut with modest pressure and allowed to heal at room temperature for 48 h. Upon retesting, the healing efficiency as measured by the recovery of interlaminar fracture toughness was found to be about 38% on average with a maximum of nearly 45%. By elevating the healing temperature to 80 °C, the healing efficiency increased to 66% on average with a maximum of over 80%. Experimental controls were tested in which the healing agent was manually injected yielding 100% recovery, and where only the catalyst was included in the polymer matrix giving 73% recovery on average.

While the repair of large scale delaminations have been shown to be feasible with the current materials system, the targeted applications for self-healing are on a much smaller scale. An important step forward in self-healing research is the development of smaller microcapsules distributed throughout the entire matrix phase and the evaluation of healing under fatigue loading conditions. Small-scale microcracking that appears in the matrix phase under repeated thermomechanical loading eventually leads to large-scale damage (e.g. delamination). Healing of microcracks could delay or prevent large-scale damage in structural composites.

Acknowledgements

Funding for this work has been provided by the AFOSR Aerospace and Materials Science Directorate (F49620-00-1-0094) and by a Graduate Fellowship from the Beckman Institute for Advanced Science and Technology at the University of Illinois at Urbana-Champaign. Electron microscopy was carried out in the Center for Microanalysis of Materials, University of Illinois, which is supported by the US Department of Energy. The authors would like to thank Mr Jon Young for his help with specimen manufacturing and testing. The authors gratefully acknowledge the technical advice and guidance of Professors Jeffrey Moore, Philippe Geubelle, and Paul Braun and to Mr Eric Brown and Dr Suresh Sriram throughout this investigation.

References

[1] Talrega R. Damage development in composites: mechanisms and modelling. J Strain Anal Engng Des 1989;24:215–22.
[2] Talrega R, editor. Damage mechanics of composite materials. New York: Elsevier; 1994.
[3] Gamstedt EK, Talrega R. Fatigue damage mechanisms in unidirectional carbon-fibre-reinforced plastics. J Mater Sci 1999;34:2535–46.
[4] Hollaway L. Polymer composites for civil and structural engineering. London: Chapman & Hall; 1993.
[5] Heslehurst RB. Challenges in the repair of composite structures—Part I. SAMPE J 1997;33(5):11–16.
[6] Heslehurst RB. Challenges in the repair of composite structures—Part II. SAMPE J 1997;33(6):16–21.
[7] Liu D, Lee CY, Lu X. Repairability of impact-induced damage in SMC composites. J Compos Mater 1993;27(13):1257–70.
[8] Mahler M, Hahn HT. In Eighth Japan-US Conference on Composite Materials, Baltimore, Md, September 24–25, 1998. Proceedings (A99-19426 04-24).Lancaster, Pa: Technomic Publishing Co. Inc; 1998. p. 53–62.
[9] Russell AJ, Bowers CP. Resin requirements for successful repair of delaminations. In 36th International SAMPE Symposium, San Diego, CA; April 15–18, 1991. p. 2279–91.
[10] Dehm S, Wurzel D. Fast in-situ repair of aircraft panel components. J Aircraft 1989;26(5):476–81.
[11] Heslehurst RB. Repair of delamination damage–a simplified approach. Int SAMPE Symp Exhibition 1996;41(2):915–24.
[12] Suchar-Buell KJ. Structural repair of composites. Polym Polym Compos 1993;1(4):297–308.
[13] White SR, Sottos NR, Geubelle PH, Moore JS, Kessler MR, Sriram SR, Brown EN, Viswanathan S. Autonomic healing of polymer composites. Nature 2001;409:794–7.
[14] Brown EN, Sottos NR, White SR. Fracture testing of a self-healing polymer composite. Exp Mech 2002;42(4):372–9.
[15] Kessler MR, White SR. Self-activated healing of delamination damage in woven composites. Composites Part A: Appl Sci Manuf 2001;32:683–99.
[16] Kessler MR. Characterization and performance of a self-healing composite material. PhD Dissertation. University of Illinois at Urbana-Champaign; 2002.
[17] Mostovoy S. 10th Interim Report, LR27614-10, Contract F 33615-75-C-5224, AFML; 1975.
[18] Brussat TR, Chin ST, Mostovoy S. Fracture mechanics for structural adhesive bonds. Phase II, AFML-TR-77-163. Wright-Patterson Air Force Base. Ohio; 1978.

[19] Bandyopadhyay S, Gellert EP, Silva VM, Underwood JH. Microscopic aspects of failure and fracture in cross-ply fibre reinforced composite laminates. J Compos Mater 1989;23:1216–31.
[20] Bascom WD, Bitner JL, Moulton RJ, Siebert AR. The interlaminar fracture of organic-matrix, woven reinforcement composites. Composites 1980;11(1):9–18.
[21] Hwang W, Han KS. Interlaminar fracture behavior and fiber bridging of glass-epoxy composite under mode I static and cyclic loadings. J Compos Mater 1989;23:396–430.
[22] Smith G, Green AK, Bowyer WH. The fracture toughness of glass fabric reinforced polyester resins. In: Stanley P, editor. Fracture mechanics in engineering practice. London: Applied Science Publishers Ltd; 1976. p. 271–87.
[23] Daniel IM, Shareef I, Aliyu AA. Rate effects on delamination fracture toughness of a toughened graphite/epoxy. In: Johnston NJ, editor. Toughened composites. ASTM STP. American Society for Testing and Materials; 1987. p. 260–74.
[24] Zhu XY, Li ZX, Jin YX. Laminar fracture behaviour of (carbon/glass) hybrid fibre reinforced laminates. Part I. Laminar fracture process. Engng Fract Mech 1993;44(4):545–52.
[25] Han KS, Koutski J. The interlaminar fracture energy of glass fiber reinforced polyester composites. J Compos Mater 1981;15:371–88.
[26] Bascom WD, Boll DJ, Hunston DL, Fuller B, Phillips PJ. Fractographic analysis of interlaminar fracture. In: Johnston NJ, editor. Toughened composites. ASTM STP. American Society for Testing and Materials; 1987. p. 131–49.
[27] Lee SM. A comparison of fracture toughness of matrix controlled failure modes: delamination and transverse cracking. J Compos Mater 1986;20:185–96.
[28] Li Z, Zhou J, Ding M, He T. A study of the effect of geometry on the mode I interlaminar fracture toughness measured by width tapered double cantilever beam specimen. J Mater Sci Lett 1996;15:1489–91.
[29] Ebeling T, Hiltner A, Baer E. Delamination failure of a woven glass fiber composite. J Compos Mater 1997;31(13):1318–33.
[30] Hirai Y, Hamada H. Determination of interfacial material constants in plain glass woven fabric using finite element analysis. Compos Interfaces 1997;5(1):69–86.
[31] Suzuki Y, Maekawa Z, Hamada H, Yokoyama A, Sugihara T, Hojo M. Influence of silane coupling agents on interlaminar fracture in glass fibre fabric reinforced unsaturated polyester laminates. J Mater Sci 1993;28(7):1725–32.
[32] Martin RH. Delamination characterization of woven glass/polyester composites. J Compos Technol Res 1997;19(1):20–8.
[33] Drzal LT, Madhukar M. Fiber–matrix adhesion and its relationship to composite mechanical properties. J Mater Sci 1993;28(3):569–610.
[34] Bradley WL, Cohen RN. Matrix deformation and fracture in graphite-reinforced epoxies. Delamination and debonding of materials. ASTM STP 876. American Society for Testing and Materials; 1985. p. 389–410.
[35] Kessler MR, White SR. Cure kinetics of ring-opening metathesis polymerization of dicyclopentadiene. J Polym Sci, Part A 2002;40:2373–83.